JOURNAL OF NEUROTRAUMA
Volume 18, Number 5, 2001
Mary Ann Liebert, Inc.

Dynamic Stretch Correlates to Both Morphological Abnormalities and Electrophysiological Impairment in a Model of Traumatic Axonal Injury

ALLISON C. BAIN,[1] RAMESH RAGHUPATHI,[2] and DAVID F. MEANEY[1]

ABSTRACT

In this investigation, the relationships between stretch and both morphological and electrophysiological signs of axonal injury were examined in the guinea pig optic nerve stretch model. Additionally, the relationship between axonal morphology and electrophysiological impairment was assessed. Axonal injury was produced *in vivo* by elongating the guinea pig optic nerve between 0 and 8 mm ($N_{total} = 70$). Morphological damage was detected using neurofilament immunohistochemistry (SMI 32). Electrophysiological impairment was determined using changes in visual evoked potentials (VEPs) measured prior to injury, every 5 min for 40 min following injury, and at sacrifice (72 h). All nerves subjected to ocular displacements greater than 6 mm demonstrated axonal swellings and retraction bulbs, while nerves subjected to displacements below 4 mm did not show any signs of morphological injury. Planned comparisons of latency shifts of the N_{35} peak in the VEPs showed that ocular displacements greater than 5 mm produced electrophysiological impairment that was significantly different from sham animals. Logit analysis demonstrated that less stretch was required to elicit electrophysiological changes (5.5 mm) than morphological signs of damage (6.8 mm). Moreover, Student *t* tests indicated that the mean latency shift measured in animals exhibiting morphological injury was significantly greater than that calculated from animals lacking morphological injury ($p < 0.01$). These data show that distinct mechanical thresholds exist for both morphological and electrophysiological damage to the white matter. In a larger context, the distinct injury thresholds presented in the report will aid in the biomechanical assessment of animate models of head injury, as well as assist in extending these findings to predict the conditions that cause white matter injury in humans.

Key words: axonal injury; biomechanics; injury tolerance; stretch injury; head injury

INTRODUCTION

DIFFUSE AXONAL INJURY (DAI) refers to a hallmark pathology in human patients with diffuse brain injuries. Morphologically, the central feature of DAI is microscopic damage to axons throughout the white matter of the brain. In its mildest form, no visible, macroscopic evidence of injury is present; diffuse damage, most prominent in the corpus callosum and parasagittal white matter, must be examined histologically. In the most severe cases of human DAI, increasing damage to axons in both cerebral hemispheres is accompanied by visible, fo-

Departments of [1]Bioengineering and [2]Neurosurgery, University of Pennsylvania, Philadelphia, Pennsylvania.

cal lesions in the corpus callosum. The neurological sequelae of DAI is frequently characterized by immediate unconsciousness that varies in duration depending on the severity of the injury. Patients with mild DAI usually exhibit an immediate, reversible concussion with unconsciousness rarely exceeding 2 h and often as short as 5 min. In severe forms of DAI, prolonged unconsciousness or coma lasts for more than 24 h and the patient usually exhibits decortication and/or decerebration indicative of brainstem dysfunction. These patients either remain in a permanent, vegetative state or, more commonly, die as a result of their injury (Strich, 1956; Nevin, 1967; Peerless and Rewcastle, 1967; Oppenheimer, 1968; Adams et al., 1981; Gennarelli et al., 1982; Gennarelli, 1983; Pilz, 1983; Vanezis et al., 1987).

Although DAI has received considerable attention in the past, many biomechanical aspects of DAI have not yet been characterized completely. A major unresolved issue is the determination of the mechanical criteria for axonal damage and assessing if the same mechanical threshold for damage applies for both morphological and functional measures of injury. Assigning a mechanical criteria for "injury" in white matter tissue—either structural damage or functional changes in the tissue—can assist in developing a better understanding of how animal and computational models can faithfully replicate the distribution of axonal damage observed in human closed head injury, as well as replicating the different severity levels of axonal damage that is observed in humans. Knowledge of the conditions that cause axonal damage *in vivo* can also guide the future development of animal models, providing one with a set of mechanical conditions that need to be reproduced to create axonal damage.

As a means to better understand the mechanical criteria for *in vivo* axonal injury, a simple model of isolated axonal injury—dynamic uniaxial elongation of the guinea pig optic nerve—has been developed (Gennarelli et al., 1989). Unlike optic nerve crush and transection (Misantone et al., 1984; Duvdevani et al., 1990; Sabel and Aschoff, 1993), which have aided in understanding the consequences of severe axonal damage and complete tissue tears, uniaxial elongation of the optic nerve mimics the primary, dynamic mechanism responsible for human axonal injury, and also facilitates the study of mild and moderate degrees of axonal injury. Previous investigations using this model have greatly improved our understanding of the sequence of neurochemical and ultrastructural events that lead to axonal injury, but do not address the specific biomechanical parameters necessary to produce axonal injury. Specifically, although it is now generally accepted that strain is the primary mechanical mediator of axonal injury, the changes in axon morphology and function caused by different levels of stretch have not yet been evaluated. Furthermore, no studies have addressed the potential relationship between axon morphology and a quantitative measure of function.

In this investigation, we examine the stretch–response relationships for morphological and electrophysiological changes in the guinea pig optic nerve stretch model. We describe changes in the structure and function of the optic nerve at discrete levels of stretch, and define the specific stretch levels necessary to produce consistent changes in structure and function. Lastly, we compare the functional response to the measured morphological changes in each stretched optic nerve, assessing if a measured latency in visual evoked potential can be a useful predictor of morphological changes in the same optic nerve.

METHODS

Optic Nerve Injury Device

The optic nerve injury device used in this study has been previously described (Bain and Meaney, 2000; Maxwell et al., 1999) and is distinct from the device used in initial studies with this model (Gennarelli et al., 1989). Briefly, the device used here delivers a reproducible, measurable amount of uniaxial displacement (0–10 mm) over a prescribed duration (60 msec, strain rate $\approx$ 30–60/sec). Ocular displacement is actuated by a solenoid that is triggered by an electronic circuit and is measured by a linear variable differential transformer (LVDT; Trans-Tek Inc., Ellington, CT) connected in parallel with the solenoid. The magnitude of the displacement is controlled by a micromanipulator that adjusts the distance traveled by the solenoid piston.

Animal Surgery and Injury

Adult, male, Hartley albino guinea pigs (600–700 g) were anesthetized with a mixture of ketamine (50 mg/mL) and xylazine (5 mg/mL). The right upper and lower eyelids were injected at the canthi with 2% lidocaine and were retracted with suture. Using iris scissors, a 360° opening was made in the conjunctiva of the right eye, and the six extraocular muscle insertions were severed. A sling constructed of sterile surgical material was placed around the posterior side of the globe so that the optic nerve projected through a slit in the sling. The animal was placed in the optic nerve injury device stereotaxic head holder angled at 45° to align the right optic nerve in the direction of displacement. The free ends of the sling were connected to the injury device. The nerve was slightly preloaded (2 g) to remove any slack. The

micromanipulator was adjusted to prescribe the magnitude of ocular displacement. Six displacement levels (3, 4, 5, 6, 7, and 8 mm) were examined, with 10 animals injured within each displacement group. Each animal received a single stretch injury, and an additional group of 10 animals served as surgical sham controls. Following stretch, the sling was cut free from the force transducer, the animal was removed from the stereotaxic head holder, and the sling was removed from the globe. The animal was monitored until it was completely ambulatory and was then returned to the animal facility. All surgical techniques were approved by the University of Pennsylvania's Institute for Animal Care and Use Committee (IACUC).

Measurement of Visual Evoked Potentials

The functional impairment of the optic nerve was assessed using electrical potentials generated by the retinal ganglion cells and transmitted, via the optic nerve, to the occipital cortex of the brain. The positive and negative peaks that make up a visual evoked potential (VEP) occur at specific time intervals after a light stimulus. Functional impairment of the optic nerve is indicated by an increase in the latency of these individual peaks. A VEP assesses the overall function of all the axons in the nerve. A latent VEP may either be indicative of a proportion of axons producing diminished electrical potentials or all of the axons exhibiting some impairment (Sokol, 1976; Harding, 1984; Mahapatra and Bhatia, 1989; Tomei et al., 1990). The methods used to measure VEPs have been described previously (Bain and Meaney, 2000). Briefly, the scalp was shaved and the scalp, left ear, and right foot were cleaned with isopropyl alcohol prior to surgery. Two sterile needle electrodes were inserted under the scalp over the left and right visual cortex—5 mm lateral to the midline and 2 mm anterior to the lambda. The majority of axons in the albino guinea pig optic nerve (~97%) cross at the optic chiasm and traverse to the contralateral visual cortex (Creel, 1972; Creel et al., 1973; Ducati et al., 1988; Gennarelli et al., 1989). Hence, VEPs originating from the right optic nerve are measured by the electrode at the left visual cortex. A third reference electrode was coated with electrode gel and clipped to the left ear. A ground electrode was attached to the right foot. The animal was placed in a grounded Faraday cage and the electrodes were inserted into the electrode panel. To improve the signal-to-noise ratio, the guinea pig was dark adapted for 4 min prior to each set of VEP measurements (Suzuki et al., 1991a,b). After dark adaptation, a photostimulator presented unpatterned flashes from a lamp placed 20 cm from the right eye at a rate of 1.0 Hz (Grass Instruments, Astro-Med, Inc., West Warwick, RI). The flash was directed at the right eye via a black cone placed over the lamp that prevented the left eye from being stimulated. Each flash elicited a VEP from the injured nerve and was measured at the left visual cortex. Each signal was preamplified (×1,000) and measured for 500 msec postflash. For each recording time point, one set of 64 VEPs (one VEP per flash) were recorded by a computer-based data acquisition system (2 kHz sampling rate). The set of 64 VEPs was averaged to produce a final VEP recording.

Three sets of control VEPs were measured prior to the surgical preparations and injury. After injury, the animal was quickly removed from the injury apparatus, the sling was removed, the animal was immediately placed in the Faraday cage, and the guinea pig was dark adapted. This process required approximately 8 min; therefore, the first recorded set of VEPs occurred at 8 min poststretch. Allowing for dark adaptation after each VEP recording, subsequent poststretch VEPs were recorded every 5 min, ending at 48 min, and then again at sacrifice (72 h). Five animals within each displacement group were monitored poststretch.

Immunohistochemistry and Morphological Injury Threshold

At three days poststretch, the animal was euthanized with a lethal dose of sodium pentobarbital (60 mg/kg), exsanguinated with 0.1% heparinized saline, and perfused with 10% neutral buffered formalin followed by 10% sucrose saline. Both left and right optic nerves were removed and postfixed in 10% neutral buffered formalin for 24 h, with the left (unstretched) serving as controls. The optic nerves were then dissected free of extraocular muscles, glandular tissue, and dural sheaths and stored in 30% sucrose saline.

Each nerve was cut on a freezing microtome into two sets of longitudinal sections 16 μm thick (approximately 15 sections per set), and stored in phosphate buffered saline (PBS) for no longer than 24 h. One set of sections from each nerve was stained using the antibody SMI 32 (1:1,000 dilution, Sternberger Monoclonals, Inc., Baltimore, MD), which stains nonphosphorylated medium and heavy-chain neurofilament proteins (160 and 200 kD), respectively. All sections were mounted on slides, coverslipped, and examined visually for morphological injury with light microscopy using a ×40 objective.

Each nerve was given an injury score of 1 or 0 based on the presence (1) or absence (0) of axonal swellings and retraction bulbs in any section of the nerve. Scores were plotted versus the applied ocular displacement and analyzed with logistic regression to evaluate the relationship between ocular displacement and morphological injury (SYSTAT LOGIT Plug-in Module, SPSS Inc.,

Chicago, IL). From this analysis, we determined the 50th percentile threshold value for the onset of morphological injury, as well as the 95th percentile value. These thresholds correspond to the displacement level at which injury is exhibited in half of the nerves and almost all nerves.

Peak Latency Shift Analysis

All signals were digitally filtered with a Chebyshev 1–100-Hz bandpass filter (Matlab, Mathworks, Inc., Natick, MA). Electrophysiological impairment can be characterized by either changes in the amplitude or latency of the individual peaks of the VEP. Although both effects have been shown to indicate optic nerve dysfunction, amplitude changes are less reliable and less reproducible due to the significant amplification of the signal that is required (Sokol, 1976; Mahapatra and Bhatia, 1989). Therefore, we chose to focus on evaluating the change in peak latency. The negative peak that occurs at approximately 35 msec after the initial stimulus (N_{35}) was chosen for analysis because it was easily distinguished in all signals due to the large amplitude of the peak, and because the latency of this peak from the initial flash stimulus was consistent among animals. For each signal, the latency shift of the N_{35} peak, defined as the increase in latency from the preinjury level, was recorded. A one-way ANOVA was employed to determine if the latency shifts measured from the seven stretch groups were statistically different at the 10 recording time points (Statistica, Statsoft, Inc., Tulsa, OK). Planned comparisons were used to detect significant differences between the groups. For all tests, significance levels were set at $p < 0.05$.

As with our morphological injury analysis, we assigned a functional injury status to each nerve at every time point based on the magnitude of the measured latency shift. The mean and standard deviation of the latency of the N_{35} peak in VEPs measured from control animals were calculated and used to define presence or absence of functional injury. All latency recordings that fell outside two standard deviations of the average sham latency were labeled as injured (1); all other recordings were considered uninjured (0). At each time point, logistic regression analysis was employed to determine the 50th and 95th percentile ocular displacement thresholds for electrophysiological impairment.

Comparison of Morphology and Electrophysiology

At each time point, the latency shift measurements were separated into two groups: (1) measurements from animals that exhibited morphological injury and (2) measurements from animals in which SMI-32 immunohistochemistry did not detect morphological injury. Student *t* tests were used at each time point to detect significant differences between the latency shifts for these two groups. The significance level was set at $p < 0.05$.

To evaluate the ability of the latency in the visual evoked potential to predict morphological injury, we calculated the positive predictive value (PPV) and the negative predictive value (NPV) of the VEP measurements (Einstein et al., 1997). First, we constructed a "truth table" based on a comparison of the morphological injury status to the functional injury status for each experiment (Altman, 1991). The truth table consists of four categories—true positives (TP), false positives (FP), false negatives (FN), and true negatives (TN). Each experiment falls into one category depending on whether or not the VEP recording demonstrated injury and whether or not the animal exhibited morphological signs of injury. The PPV is based on the number of true positives (morphological injury = 1; functional injury = 1) and false positives (morphological injury = 0; functional injury = 1) in the data set (equation 1). The NPV is based on the number of false negatives (morphological injury = 1; functional injury = 0) and true negatives (morphological injury = 0; functional injury = 0; equation 2).

$$PPV = \frac{TP}{TP + FP} \tag{1}$$

$$NPV = \frac{TN}{TN + FN} \tag{2}$$

Together, these measures provide an assessment of the efficacy of the chosen measure in practice. The closer PPV and NPV are to 1.0, the better the predictive measure is in practice. Ideally, the predictor should achieve high values of both PPV and NPV.

Both PPV and NPV were calculated at each time point to determine the optimal recording time for using VEPs as predictive measures of morphological damage. We defined our "optimal" recording time as the time point at which the sum of PPV and NPV was maximized (Connell and Koepsell, 1985).

RESULTS

Morphological Injury

Of the 70 *in vivo* experiments, morphological injury was detected in 33 of the nerves. Evidence of axonal injury was first noted in one of the animals injured at an ocular displacement of 4 mm. In this case, low numbers of both axonal swellings (<5 per nerve section) and retraction bulbs (<5 per nerve section) were observed

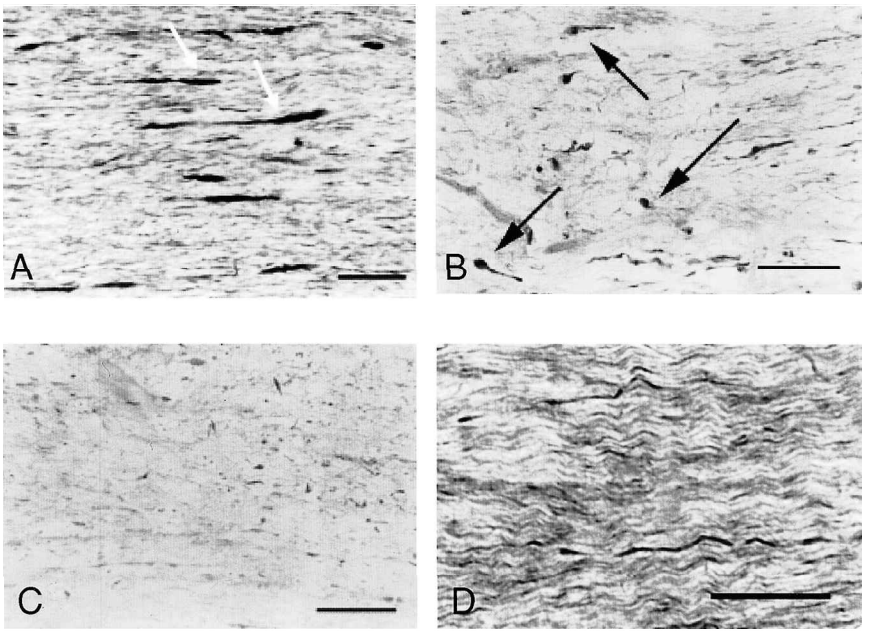

FIG. 1. Immunohistochemistry of longitudinal optic nerve sections at the 72-h survival time. **(A,B)** Longitudinal optic nerve sections were injured using a 7-mm displacement and stained with SMI32, a marker for nonphosphorylated medium and heavy weight neurofilament proteins. Injured nerves show clusters of retraction bulbs (black arrows) and axonal swellings (white arrows) 1–3 mm from the retina and 1–2 mm from the chiasm. **(C)** Longitudinal section from a nerve stretch at the highest displacement level, with noticeable axonal degeneration fragments. **(D)** Unstretched surgical sham Bar = 40 μm.

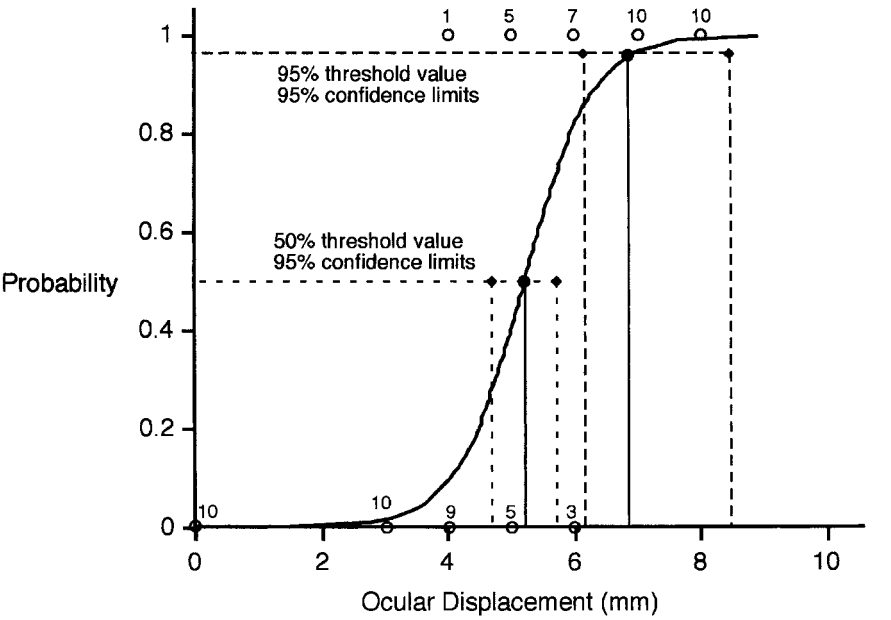

FIG. 2. Logistic regression analysis of morphological injury data. Each nerve was given an injury score of 1 or 0 based on the presence (1) or absence (0) of axonal swellings and retraction bulbs in any section of the nerve. Scores were plotted versus the applied ocular displacement and analyzed with logistic regression to evaluate the relationship between ocular displacement and morphological injury. Numbers above the open circles represent the number of animals in which morphological injury was detected (probability = 1) or not detected (probability = 0) at each level of ocular displacement. The logit analysis (line) predicted a 50th percentile threshold displacement (●) of 5.2 mm with 95% confidence limits (◆) of 4.7 and 5.7 mm. In comparison, a 95% morphological injury threshold limit of 6.8 mm was predicted with the logit fit, with 95% confidence limits of 6.1 and 8.4 mm.

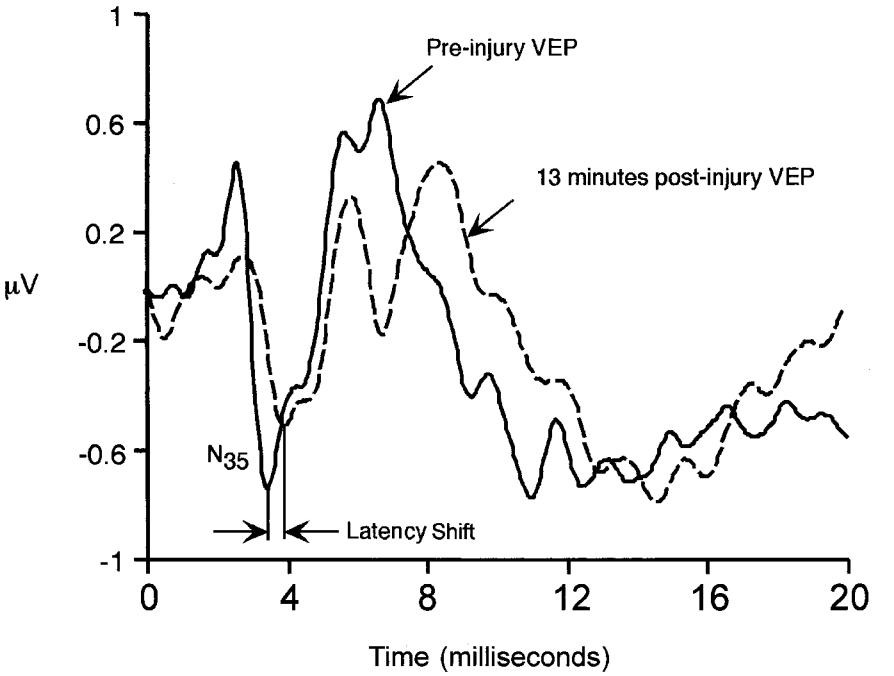

FIG. 3. Typical visual evoked potential (VEP) traces recorded at the left visual cortex before (solid line) and 13 min after the right nerve was subjected to a 6-mm stretch (dashed line). Electrophysiological impairment was based on the magnitude of the latency shift—defined as the increase in latency from the preinjury levels—observed in the large negative peak that occurs at approximately 35 msec.

within 1–3 mm from the retina. Axonal swellings were characterized by variable increases in the caliber of the axon that sometimes appeared several times in a single axon (Fig. 1A). Retraction bulbs were distinguished by a characteristic elongated, bulbous shape attached to a much smaller caliber tail (Fig. 1B). As the stretch level was increased, the density of axonal abnormalities near the retina increased, and axonal pathology started to appear in clusters 1–2 mm from the chiasm. At the highest stretch levels, isolated retraction bulbs and axonal degeneration fragments were also frequently found along the length of injured nerves (Fig. 1C). In comparison, no swellings or degeneration fragments were observed in surgical sham tissue (Fig. 1D).

When morphological injury status was compared to applied ocular displacement, the coefficients of the logistic regression model were estimated with very high significance (Likelihood Ratio test, χ^2, $p < 0.0001$). McFadden's rho-squared term, similar to the correlation coefficient in linear regression, was also highly significant (0.640; Heshner and Johnson, 1981; Steinberg and Colla 1991). Based on the logit analysis, half of all nerves stretched at 5.2 mm (95% confidence limits: 4.7, 5.7 mm) would demonstrate morphological injury (Fig. 2). Also, the logit analysis predicted a minimum stretch of 6.8 mm stretch to achieve axonal injury consistently in this model, that is, in more than 95% of all animals receiving stretch.

Electrophysiological Impairment

Normal, prestretch VEPs were consistent among animals and between preinjury trials. The typical waveform compared very well to those recorded by other investigators, and was composed of three low amplitude positive peaks between 5 and 30 msec, a large amplitude negative peak at approximately 35 msec, and one (sometimes two) positive peaks between 65 and 100 msec (Fig. 3). The mean latency (±SD) of the N_{35} peak from the initial flash stimulus in prestretch recordings was 34.8 ± 1.1 msec.

At all levels of ocular displacement, electrophysiological impairment of the optic nerve was noted at the earliest time point after injury (8 min), as indicated by a latency shift of the N_{35} peak (Fig. 4). Nerves injured at higher levels of ocular displacement generally showed greater shift in N_{35} latency. In most cases, N_{35} latency shifts gradually decreased after injury, and returned to preinjury levels by 72 h. At all time points except 72 h, N_{35} latency shifts were significantly different among the seven groups (0, 3, 4, 5, 6, 7, and 8 mm ocular dis-

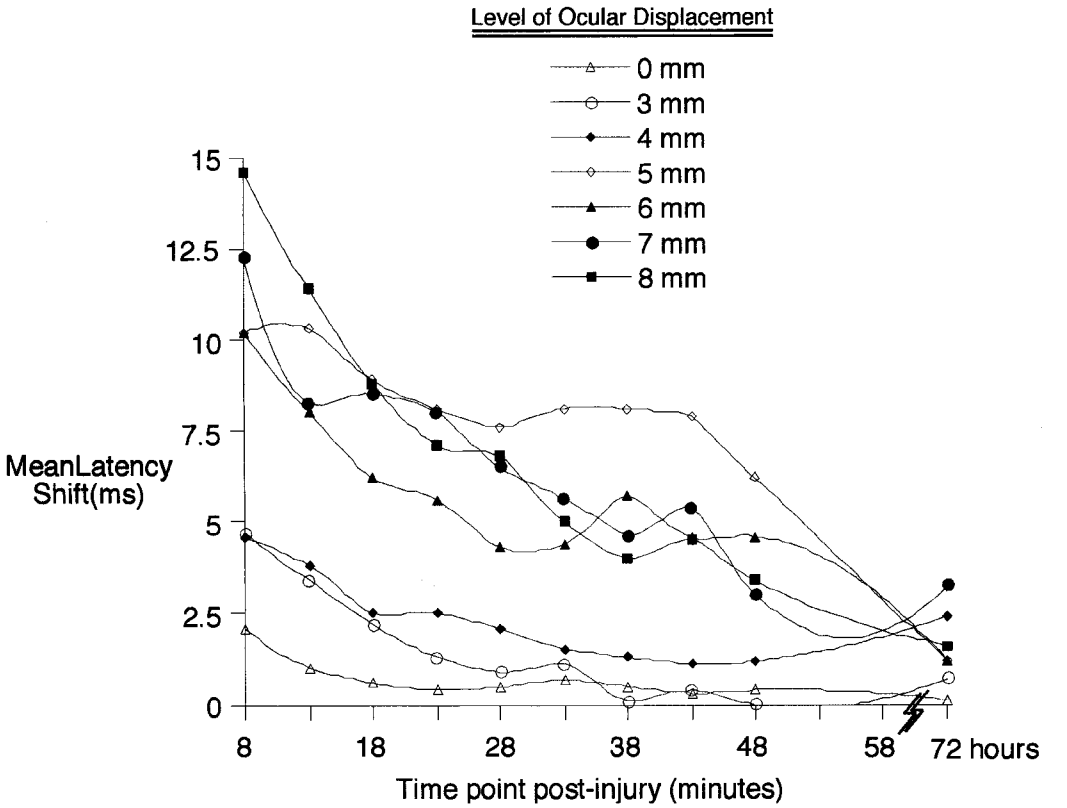

FIG. 4. Mean latency shifts of the N_{35} peak calculated for each stretch level at all recorded time points poststretch. Latency shift is defined as the increase in latency (time of occurrence) from the preinjury levels. Within naive control animals, the average latency shift was 34.8 ± 1.1 msec. At all levels of stretch ($N_{level} = 5$), a shift in the latency of the N_{35} peak was observed at the earliest time point after stretch (8 min). At the earliest time point, the mean latency shifts increased in proportion to the applied stretch level. A-one way ANOVA demonstrated the latency shifts measured in the 5, 6, 7, and 8 mm stretch groups were significantly different from sham animals at all time points except 48 min and 72 h ($p < 0.05$).

placements; ANOVA, $p < 0.05$). Also, planned comparisons showed that latency shifts measured in animals injured with a 5, 6, 7, and 8 mm stretch were significantly different from sham animals ($p < 0.05$) at all time points except 48 min and 72 h. However, there were no significant differences detected in animals injured with a 3 or 4 mm stretch when compared to sham animals.

At all time points except 48 min and 72 h, the coefficients of the logistic regression models were estimated with high significance (Likelihood Ratio test, χ^2, $p < 0.0001$). Also, McFadden's rho-squared values were very high at these same time points. At the earliest possible recording time point, logistic regression analysis predicted that half of all nerves subjected to a 3.0-mm stretch would show functional injury. Nearly all of the nerves (95%) will show changes in the VEP recorded at this time point when subjected to a 5.5-mm stretch. These stretch levels generally increased with time poststretch due to a recovery of the VEP waveforms over time. Stretch levels necessary to induce a significant latency in the N_{35} peak in half of the nerves increased to 4.7 mm at 43 min, while the stretch level required to achieve consistent impairment (>95% of all animals) in the VEPs reached a peak value of 7.3 mm at 33 and 38 min (Fig. 5). The logit analysis did not yield statistically significant terms at 48 min and 72 h; therefore, no threshold values were determined for these recording time points.

Comparison of Morphology and Electrophysiology

Student t tests indicated that, at all time points, the mean latency shift of the N_{35} peak measured in animals exhibiting morphological evidence of axonal injury was significantly greater than that calculated from animals lacking morphological injury ($p < 0.05$). Also, injured and uninjured mean latency shifts decreased progressively after injury (Fig. 6).

When morphological injury status was compared to functional injury status, the calculated PPV and NPV

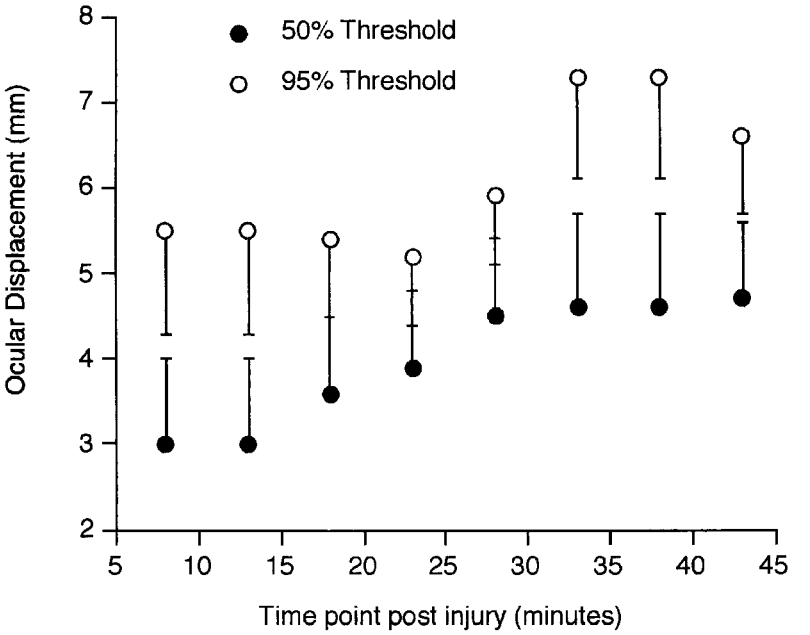

FIG. 5. The 50th and 95th percentile displacement thresholds, predicted from logistic regression, for electrophysiological impairment. Each treated nerve was scored as either having a significant electrophysiological impairment (score = 1) or no detectable impairment (score = 0), based on whether or not the latency shift fell outside two standard deviations of the average latency measured in control animals. In general, the thresholds increased with time post injury as most visual evoked potentials recovered to prestretch shape. The 50% threshold (●, bar: 95% confidence interval) increased from 2.9 mm at 8 min after stretch to 4.7 mm at 43 min. Similarly, the displacement threshold for impairment in 95% of animals (○, bar = 95% confidence interval) ranged from 5.2 mm at 23 min to 7.3 mm stretch at 33 and 38 min poststretch.

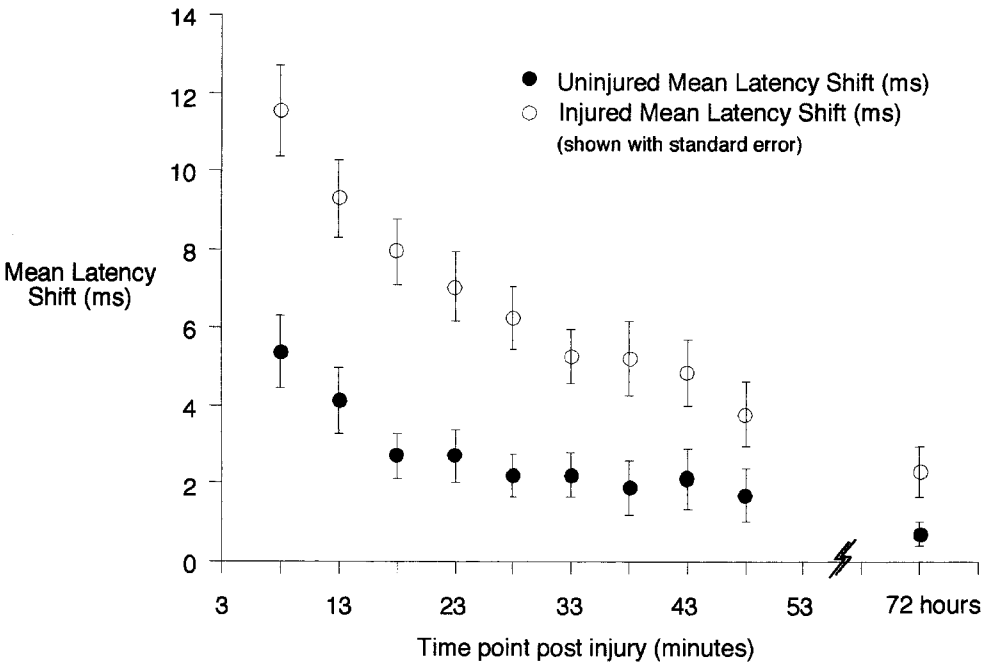

FIG. 6. The mean latency shift of all optic nerves showing morphological changes with SMI 32 (○) was significantly different ($p < 0.05$) than the mean latency of nerves not showing morphological changes (●) across all time points.

ranged from 0.60 to 0.925 (Fig. 7). In general, PPV values gradually increased as time postinjury increased and NPV values primarily decreased with increasing time. Overall, the highest PPV was achieved with data recorded at 23 min after injury, and the highest NPV value was reached with recordings at 28 min postinjury. These results suggest that the optimal time point for recording VEPs and for using latency shift measurements as predictors of morphological damage is approximately 25–30 min after injury.

DISCUSSION

In this investigation, the biomechanics of stretch-induced axonal injury was quantified, relating the magnitude of the stretch insult to both the presence of morphological changes and the changes in latency of the visual evoked potential. Morphological injury, detected by changes in neurofilament immunoreactivity, exhibited a graded response as the stretch level was increased. Similarly, peak latency shifts measured from pre- and postinjury VEPs revealed that electrophysiological impairment gradually increased with increasing stretch levels. Interestingly, there was a significant difference between mean latency shift measured in animals demonstrating morphological injury compared to animals lacking morphological injury. Although statistically different at all time points, this difference was most prominent at early time points and progressively decreased with increasing time poststretch. This investigation is the first to examine stretch-dependent changes in axon morphology and function in an in vivo model of axonal injury, and is the first quantitative combination of functional axonal injury and immunohistochemical information in an attempt to relate the existence of morphological injury to the functional impairment of the tissue in white matter injury.

The axonal pathology in our experiments compares well with other investigations using this model of axonal injury. Gennarelli et al. (1989) and Tomei et al. (1990) both observed retraction bulbs and axonal swellings using a horseradish peroxidase marker that were similar in appearance and in location to those observed in this study. Although retraction bulbs detected in axonal injury models using the pig and nonhuman primate subjected to inertial brain injury appeared slightly more spherical in shape, the relative caliber was similar and axonal swellings were very similar in appearance (Adams et al., 1981; Gennarelli et al., 1982; Ross et al., 1994; Smith et al., 1997). Most importantly, the general axonal pathology seen in this model is similar to what is observed in human axonal injury (Strich, 1956; Adams et al., 1982; Blumbergs et al., 1989; Povlishock, 1993); that is, parts of the nerve exhibit different types of axonal injury (swellings versus retraction bulbs) and a majority of axons appear morphologically uninjured.

Despite such similarities among the investigations using the optic nerve stretch model, it is important to note

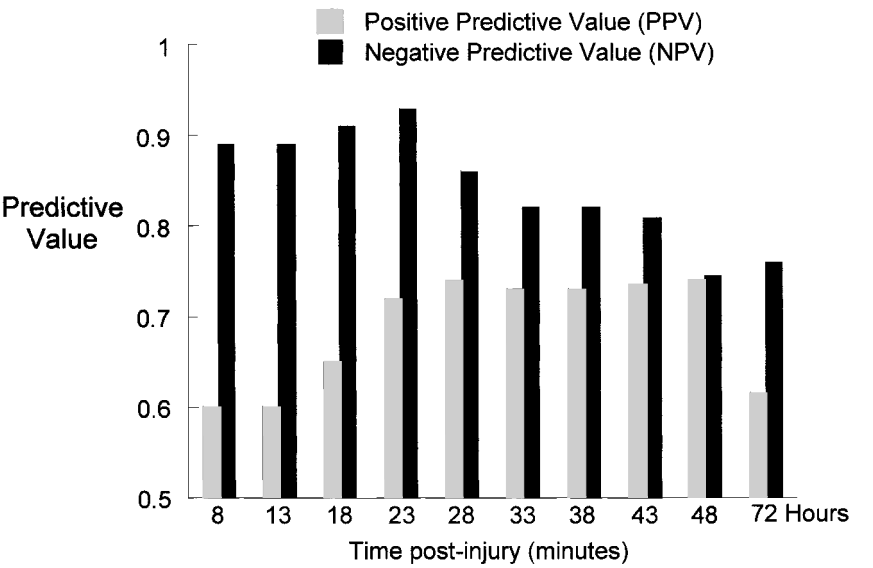

FIG. 7. Positive predictive value (PPV) and negative predictive value (NPV) calculated at the different time points when electrophysiological impairment was compared to morphological injury. In general, PPV increased over time, while NPV decreased. Both values reached peak levels at 25–30 min postinjury. These values were used to assess the ability of the latency shift measurements to predict presence of morphological injury.

our study extends previous investigations in two areas: we examined the dose–response relationship for this model, and we evaluated the use of a functional measure as a prognostic indicator for morphological damage. Previous studies only examined a single stretch level (5 mm), with axonal pathology observed in all animals at this stretch level (Gennarelli et al., 1989; Tomei et al., 1990; Maxwell et al., 1991). In contrast, we noted mild morphological injury in only half of the animals in the 5-mm stretch group, and did not achieve morphological injury consistently until the 7-mm stretch group. We attribute this difference to the small 2-g preload used in the current study, much lower than the 40-g preload used in past investigations. The minimal preload was selected to minimize the prestretching of the optic nerve prior to the dynamic stretch insult, and will allow us to determine, in the future, the tissue strain required to cause morphological changes and functional deficits in the optic nerve. It is important to note that the magnitude of the preload affected only the presence or absence of morphological injury at a specific stretch level; once injury was produced, the axonal profiles observed did not appear significantly different than those from previous studies.

Differences in the degree and type of axonal pathology among investigations may also be due to the specific technique used to visualize injury. Currently, the most common methods involve using antibodies to stain different axonal components, such as microtubule and neurofilament proteins and amyloid precursor protein (APP), as well as visualizing injected tracers such as horseradish peroxidase (HRP) and the carbocyanine dye, diI (Rosene and Mesulam, 1978; Trojanowski, 1983; Walsh, 1986; Rosenfield et al., 1987; Gentleman et al., 1989; Honig and Hume, 1989; Price et al., 1990; Kawarabayashi et al., 1991; Yaghmai and Povlishock, 1992; Gentleman et al., 1993; Grady et al., 1993; Kawarabayashi et al., 1993; Masliah et al., 1993; Sherriff et al., 1994). Recent studies have indicated that the neurofilament protein antibodies NF 68, 160, and 200, and antibodies for APP are the most sensitive and highlight injury very clearly (Yaghmai and Povlishock, 1992; Grady et al., 1993; Sherriff et al., 1994). However, while most animal models employ rats and mice, few studies have defined procedures and protocols for using these antibodies in guinea pig CNS tissue. Preliminary studies completed for this report showed that SMI 32 performed consistently well for highlighting regions of axonal injury in damaged tissue, and produced little background staining in naïve controls. In contrast, even at very low concentrations, NF 160 and 200 produced a dark background in the tissue that prevented visualization of injury (unpublished studies). Although used successfully with this model by other investigators (Maxwell et al., 1999), attempts to detect injury with APP antibodies were also unsuccessful across a range of antibody concentrations, and thus prevented us from using this increasingly common technique.

The comparison between morphological changes and the peak latency measures produced intriguing results. Although there are various ways to evaluate functional impairment of the visual system, few are objective, quantitative assessments of axonal injury. We chose to measure the latency shift experienced by the N_{35} peak of the VEP waveform, as in a previous study (Tomei et al., 1990), since the latency of this peak in the preinjury recordings was very consistent among the different animals and between preinjury trials. Previous investigations have shown that optic nerve stretch injury in the guinea pig (5 mm, 40 g preload) produces latencies of approximately 6–10 msec within a few minutes of the stretch injury, and the VEP waveforms in a subset of animals return to preinjury levels within 24 h, with the majority still slightly abnormal (Tomei et al., 1990). In contrast, we quantified latency changes caused by varying levels of stretch, which allowed us to evaluate thresholds for electrophysiological changes. Although sham animals exhibited small changes in peak latency at the first time point following injury, these changes were most likely due to the surgical procedures employed, and were not significantly different than control latencies. Therefore, to detect changes in VEPs due solely to stretch injury, we compared VEPs from the injured animals to sham animals. In general, we noted an increase of 25 msec in latencies at the first time point following stretch at all injury levels, and an increase in the measured latency as the stretch level was increased. We also observed a gradual recovery of the peak latencies as time progressed; many latencies returned to normal, preinjury levels by sacrifice (72 h). This data supports previous observations that individual axons either exhibited transient functional impairment and ultimately recovered full function, or that the uninjured axons compensated for the injured axons, and were able to reestablish normal function (Tomei et al., 1990).

Due to the temporal recovery of the VEP waveform, the threshold for electrophysiological impairment was not unique across different time points following stretch. The optic nerve exhibited a short-term functional response that was more sensitive to lower stretch levels than morphological injury. Also, at longer durations postinjury, higher stretch levels were required to produce significant changes in function. Consequently, it may be more appropriate to define functional injury thresholds at different time points after stretch injury or to determine short-term and long-term thresholds. However, because our last VEPs were recorded at 72 h, it is not possible to deter-

mine if this recovery is only temporary, and the possibility that the nerve would show signs of functional injury at much later time points still exists.

Although we were not able to draw definitive comparisons between morphological and functional axonal injury thresholds, we did establish a distinct relationship between the existence of axonal pathology and electrophysiological impairment. This relationship was most prominent at the first time point after injury and was least obvious at very late time points. Few studies have evaluated morphological and functional outcome measures simultaneously in an in vivo animal model. Using the optic nerve stretch model, Tomei et al. (1990) found a correlation between the presence of axonal damage and changes in electrophysiology. Also, after transection of the rat optic nerve, Sugioka et al. (1995) observed that decreased fiber density correlated to increased latency of the VEP waveform. Finally, using the optic nerve crush model, Sabel and Aschoff (1993) found that functional recovery at later time points did not correlate to the degree of morphological injury at these time points.

The existence of a quantifiable relationship between morphology and function is most important due to the potential diagnostic value of functional measures with respect to morphological axonal injury. This concept has particular value in a clinical setting, where it is frequently necessary to make assessments of morphology based on the degree of functional impairment. Currently, most clinical assessments of function are based on subjective measurements. The relationship presented herein establishes promise for developing a clinical tool that can introduce a more objective diagnosis of a patient's neuropathological condition.

In a biomechanics context, the quantitative relationships developed in this study can help to better examine animal models of traumatic brain injury. Currently, investigations that focus on predicting tissue damage from the state of mechanical stress or strain within the brain parenchyma are limited by the lack of specific thresholds for injury to the white or gray matter tissues of the brain. The establishment of a dose–response relationship in the current study—relating displacement to two different forms of injury to white matter tissue—allows the transfer of findings from computational models of impact head injury into predictions of injury along white matter tracts within the brain. Followed by a rigorous validation phase for these computationally based predictions, these models can be used to develop and/or refine existing techniques to better control the distribution of damage in an animal model of traumatic brain injury, or develop new techniques to minimize the variability of an existing model of injury. The parallel development of finite element models describing the response of the human brain to impact loading will allow a similar prediction of tissue damage from applied forces or accelerations, and will develop a better insight into the specific circumstances that cause human head injury.

ACKNOWLEDGMENTS

Funds were provided by National Institutes of Health Grant NS35712 (DFM), P50-NS09903 (DFM, RR) and Centers for Disease Control Grant CDC/R49CCR312712 (DFM).

REFERENCES

ADAMS, J.H., GRAHAM, D.I., and GENNARELLI, T.A. (1981). Acceleration induced head injury in the monkey. II. Neuropathology. Acta Neuropathol. (Berl.) Suppl. **7,** 26–28.

ADAMS, J.H., GRAHAM, D.I., MURRAY, L.S., et al. (1982). Diffuse axonal injury due to nonmissile head injury in humans: an analysis of 45 cases. Ann. Neurol. **12,** 557–563.

ALTMAN, D. (1991). *Practical Statistics For Medical Research.* Chapman & Hall: New York.

BAIN, A., and MEANEY, D. (2000). Tissue-level thresholds for axonal damage in an experimental model of central nervous system white matter injury. J. Biomech. Eng. **122,** 615–622.

BLUMBERGS, P.C., JONES, N.R., and NORTH, J.B. (1989). Diffuse axonal injury in head trauma. J. Neurol. Neurosurg. Psychiatry **52,** 838–841.

CONNELL, F., and KOEPSELL, T. (1985). Measures of gain in certainty from a diagnostic test. Am. J. Epidemiol. **121,** 744–753.

CREEL, D.J. (1972). Retinogeniculostriate projections in guinea pigs: albino and pigmented strains compared. Exp. Neurol. **36,** 411–425.

CREEL, D.J., DUSTMAN, R.E., and BECK, E.C. (1973). Visually evoked responses in the rat, guinea pig, cat, monkey, and man. Exp. Neurol. **40,** 351–366.

DUCATI, A., FAVA, E., and MOTTI, E.D.F. (1988). Neuronal generators of the visual evoked potentials: intracerebral recording in awake humans. Electroencephalogr. Clin. Neurophysiol. **71,** 89–99.

DUVDEVANI, R., ROSNER, M., BELKIN, M., et al. (1990). Graded crush of the rat optic nerve as a brain injury model: combining electrophysiological and behavioral outcome. Restor. Neurol. Neurosci. **2,** 31–38.

EINSTEIN, A., BODIAN, C., and GIL, J. (1997). The relationships among performance measures in the selection of diagnostic tests. Arch. Pathol. Lab. Med. **121,** 110–117.

GENNARELLI, T.A. (1983). Head injury in man and experimental animals: clinical aspects. Acta Neurochir. Suppl. **32,** 1–13.

GENNARELLI, T.A., THIBAULT, L.E., ADAMS, J.H., et al. (1982). Diffuse axonal injury and traumatic coma in the primate. Ann. Neurol. **12,** 564–574.

GENNARELLI, T.A., THIBAULT, L.E., TIPPERMAN, R., et al. (1989). Axonal injury in the optic nerve: a model simulating diffuse injury in the brain. J. Neurosurg. **71,** 244–253.

GENTLEMAN, S.M., BRUTON, C., ALLSOP, D., et al. (1989). A demonstration of the advantages of immunostaining in the quantification of amyloid plaque deposits. Histochemistry **92,** 355–358.

GENTLEMAN, S.M., NASH, M.J., SWEETING, C.J., et al. (1993). β-Amyloid precursor protein (βAPP) as a marker for axonal injury after head injury. Neurosci. Lett. **160,** 139–144.

GRADY, M.S., McLAUGHLIN, M.R., CHRISTMAN, C.W., et al. (1993). The use of antibodies targeted against the neurofilament subunits for the detection of diffuse axonal injury in humans. J. Neuropath. Exp. Neurol. **52,** 143–152.

HARDING, G. (1984). A flash of light: a personal review of 21 years of study of the electrical activity of the visual pathway beyond the retina. Ophthalmic Physiol. Opt. **4,** 293–304.

HESHNER, D., and JOHNSON, L.W. (1981). *Applied Discrete Choice Modeling*. Croom Helm: London.

HONIG, M., and HUME, R. (1989). DiI and DiO: versatile fluorescent dyes for neuronal labeling and pathway tracing. Trends Neurosci. **12,** 333–341.

KAWARABAYASHI, T., SHOJI, M., HARIGAYA, Y., et al. (1991). Expression of APP in the early stage of brain damage. Brain Res. **563,** 334–338.

KAWARABAYASHI, T., SHOJI, M., YAMAGUCHI, H., et al. (1993). Amyloid β protein precursor accumulates in swollen neurites throughout rat brain with aging. Neurosci. Lett. **153,** 73–76.

MAHAPATRA, A.K., and BHATIA, R. (1989). Predictive value of visual evoked potentials in unilateral optic nerve injury. Surg. Neurol. **31,** 339–342.

MASLIAH, E., MALLORY, M., HANSEN, L., et al. (1993). An antibody against phosphorylated neurofilaments identifies a subset of damaged association axons in Alzheimer's disease. Am. J. Pathol. **142,** 871–882.

MAXWELL, W.L., IRVINE, A., GRAHAM, D.I., et al. (1991). Focal axonal injury: the early axonal response to stretch. J. Neurocytol. **20,** 157–164.

MAXWELL, W.L., DONNELLY, S., SUN, X., et al. (1999). Axonal cytoskeletal responses to nondisruptive axonal injury and the short-term effects of posttraumatic hypothermia. J. Neurotrauma **16,** 1225–1234.

MISANTONE, L.J., GERSHENBAUM, M., and MURRAY, M. (1984). Viability of retinal ganglion cells after optic nerve crush in adult rats. J. Neurocytol. **13,** 449–465.

NEVIN, N.C. (1967). Neuropathological changes in the white matter following head injury. J. Neuropathol. Exp. Neurol. **26,** 77–84.

OPPENHEIMER, D.R. (1968). Microscopic lesions in the brain following head injury. J. Neurol. Neurosurg. Psychiatry **31,** 299–306.

PEERLESS, S.J., and REWCASTLE, N.B. (1967). Shear injuries of the brain. Can. Med. Assoc. J. **96,** 577–582.

PILZ, P. (1983). Axonal injury in head injury. Acta Neurochir. Suppl. **32,** 119–123.

POVLISHOCK, J.T. (1993). Pathobiology of traumatically induced axonal injury in animals and man. Ann. Emerg. Med. **22,** 980–986.

PRICE, D., KOO, E., SISODIA, S., et al. (1990). Neuronal responses to injury and aging: lessons from animal models. Prog. Brain Res. **86,** 297–308.

ROSENE, D., and MESULAM, M. (1978). Fixation variables in horseradish peroxidase neurohistochemistry. I. The effects of fixation time and perfusion procedures upon enzyme activity. J. Histochem. Cytochem. **26,** 28–39.

ROSENFIELD, J., DORMAN, M.E., GRIFFIN, J.W., et al. (1987). Distribution of neurofilament antigens after axonal injury. J. Neuropathol. Exp. Neurol. **46,** 269–282.

ROSS, D.T., MEANEY, D.F., SABOL, M.K., et al. (1994). Distribution of forebrain diffuse axonal injury following inertial closed head injury in miniature swine. Exp. Neurol. **126,** 291–299.

SABEL, B.A., and ASCHOFF, A. (1993). Functional recovery and morphological changes after injury to the optic nerve. Neuropsychobiology **28,** 62–65.

SHERRIFF, F.E., BRIDGES, L.R., GENTLEMAN, S.M., et al. (1994). Markers of axonal injury in post mortem human brain. Acta Neuropathol. **88,** 433–439.

SMITH, D.H., CHEN, X.H., XU, B.N., et al. (1997). Characterization of diffuse axonal pathology and selective hippocampal damage following inertial brain trauma in the pig. J. Neuropathol. Exp. Neurol. **56,** 822–834.

SOKOL, S. (1976). Visually evoked potentials: theory, techniques and clinical applications. Surv. Ophthalmol. **21,** 18–44.

STEINBERG, D., and COLLA, P. (1991). *LOGIT: A Supplementary Module for SYSTAT.* SYSTAT, Inc.: Chicago.

STRICH, S.J. (1956). Diffuse degeneration of the cerebral white matter in severe dementia following head injury. J. Neurol. Neurosurg. Psychiatry **19,** 163–185.

SUGIOKA, M., SAWAI, H., ADACHI, E., et al. (1995). Changes of compound action potentials in retrograde axonal degeneration of rat optic nerve. Exp. Neurol. **132,** 262–270.

SUZUKI, M., SITIZYO, K., TAKEUCHI, T., et al. (1991a). Changes in the visual evoked potentials with different photic conditions in guinea pigs. J. Vet. Med. Sci. **53,** 911–915.

SUZUKI, M., SITIZYO, K., TAKEUCHI, T., et al. (1991b). Visual evoked potential from scalp in guinea pigs. J. Vet. Med. Sci. **53,** 301–305.

TOMEI, G., SPAGNOLI, D., DUCATI, A., et al. (1990). Morphology and neurophysiology of focal axonal injury experimentally induced in the guinea pig optic nerve. Acta Neuropathol. **80,** 506–513.

TROJANOWSKI, J. (1983). Time of arrival of wheat germ agglutinin-HRP conjugates in superior colliculus after intraocular injections in the rat. Brain Res. **267,** 365–370.

VANEZIS, P., CHAN, K.K., and SCHOLTZ, C.L. (1987). White matter damage following acute head injury. Forensic Sci. Int. **35,** 1–10.

WALSH, C. (1986). Age-related fiber order in the ferret's optic nerve and optic chiasm. J. Neurosci. **6,** 1635–1642.

YAGHMAI, A., and POVLISHOCK, J.T. (1992). Traumatically induced reactive change as visualized through the use of monoclonal antibodies targeted to neurofilament subunits. J. Neuropathol. Exp. Neurol. **51,** 158–176.

Address reprint requests to:
David F. Meaney, Ph.D.
Department of Bioengineering
University of Pennsylvania
3320 Smith Walk
Philadelphia, PA 19104-6392

E-mail: dmeaney@seas.upenn.edu